

This article appeared in a journal published by Elsevier. The attached copy is furnished to the author for internal non-commercial research and education use, including for instruction at the authors institution and sharing with colleagues.

Other uses, including reproduction and distribution, or selling or licensing copies, or posting to personal, institutional or third party websites are prohibited.

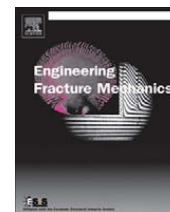
In most cases authors are permitted to post their version of the article (e.g. in Word or Tex form) to their personal website or institutional repository. Authors requiring further information regarding Elsevier's archiving and manuscript policies are encouraged to visit:

<http://www.elsevier.com/copyright>



Contents lists available at ScienceDirect

## Engineering Fracture Mechanics

journal homepage: [www.elsevier.com/locate/engfracmech](http://www.elsevier.com/locate/engfracmech)

## Mixed-mode I/II wood fracture characterization using the mixed-mode bending test

M.F.S.F. de Moura<sup>a,\*</sup>, J.M.Q. Oliveira<sup>b</sup>, J.J.L. Morais<sup>c</sup>, J. Xavier<sup>c</sup><sup>a</sup> Faculdade de Engenharia da Universidade do Porto, Departamento de Engenharia Mecânica e Gestão Industrial, Rua Dr. Roberto Frias, 4200-465 Porto, Portugal<sup>b</sup> Instituto Superior Politécnico de Viseu, Departamento de Engenharia de Madeiras, Viseu, Portugal<sup>c</sup> CITAB/UTAD, Departamento de Engenharias, Quinta de Prados, 5001-801 Vila Real, Portugal

## ARTICLE INFO

## Article history:

Received 17 January 2009

Received in revised form 16 September 2009

Accepted 28 September 2009

Available online 9 October 2009

## Keywords:

Wood

Mixed-mode fracture

Cohesive zone modelling

Civil engineering structures

## ABSTRACT

In this work fracture characterization of wood under mixed-mode I/II loading is addressed. The mixed-mode bending test is used owing to its aptitude for easier alteration of mode ratio. Experimental tests were performed covering a wide range of mode ratios in order to obtain a mixed-mode fracture criterion for the maritime pine (*Pinus pinaster* Ait.) in the RL crack propagation system. A data reduction scheme based on beam theory and crack equivalent concept was used to overcome some difficulties inherent to the test. The method does not require crack length monitoring during propagation and provide an entire resistance curve allowing easier identification of the fracture energy. A numerical analysis using cohesive elements was also performed to validate the method. The linear energetic fracture criterion was proved to be the most adequate to describe the failure envelop of this wood species.

© 2009 Elsevier Ltd. All rights reserved.

## 1. Introduction

Structural applications of wood are increasing in the last decades, which is motivated by ecological reasons and saving energy. However, its use in structural applications is still limited due to lack of adequate failure criterion. As a matter of fact, structural wood members contain natural or artificial defects such as knots and drying checks or splits; they also contain design-induced local regions with high shear or tension perpendicular to grain. On these circumstances it is globally accepted that fracture mechanics failure based criteria are more appropriate than conventional strength of materials criteria. Consequently, a considerable number of studies were recently devoted to fracture characterization of wood using fracture mechanics concepts. The majority of these works are concerned with fracture characterization under pure modes I and II [1–4]. However it should be emphasized that in the majority of real applications, wood structures behave under mixed-mode loading. These mixed-mode conditions arise from external loading and also from wood anisotropy. Wood is considered a cylindrically orthotropic material with three different directions of orthotropy: longitudinal (L) along fibers, radial (R) parallel to the rays, and tangential (T) to the growth rings. The longitudinal direction is the strongest one and the cracks tend to grow along the fibers direction independently of its initial orientation. This fracture behaviour induces mixed-mode loading conditions at the crack tip and they should be taken into account in the structural design.

Some authors have already addressed fracture characterization of wood under mixed-mode. Jernkvist [5] used the double cantilever beam (DCB) with asymmetrical arms and the single edge notched tensile (SENT) tests, whose specimens were notched with an inclination to the load direction, to investigate mixed-mode I/II loading in *Picea abies*. Tschegg et al. [6] used

\* Corresponding author. Tel.: +351 225081727; fax: +351 225081584.

E-mail address: [mfmoura@fe.up.pt](mailto:mfmoura@fe.up.pt) (M.F.S.F. de Moura).

**Nomenclature**

$a$	crack length
$a_{eqi}$	equivalent crack length in each mode $i$ ( $i = I, II$ )
$a_0$	initial crack length
$C_0$	initial compliance
$C_{0i}$	initial compliance in each mode $i$ ( $i = I, II$ )
$C$	compliance
$C_i$	compliance in each mode $i$ ( $i = I, II$ )
$c$	distance on the loading lever
$E_m$ ( $m = L, R$ )	Young's modulus
$E_{fi}$	flexural modulus in each mode $i$ ( $i = I, II$ )
$G_{LR}$	shear modulus
$\delta$	loading displacement
$\delta_C$	displacement of the specimen at the mid-span
$\delta_i$	loading displacement in each mode $i$ ( $i = I, II$ )
$\Delta_1$	crack length correction factor
$P$	applied load
$P_i$	loading component in each mode $i$ ( $i = I, II$ )
$G_i$	strain energy release rates in each mode $i$ ( $i = I, II$ )
$G_{ic}$	fracture energy in each mode $i$ ( $i = I, II$ )
$G_{Tc}$	total fracture energy under mixed-mode
$L$	half length of the specimen between supports
$L_1$	total length of the specimen
$B$	specimen width
$h$	half-height of the specimen
$\sigma_i$	stress in each mode $i$ ( $i = I, II$ )
$\sigma_{u,i}$	local strength in each mode $i$ ( $i = I, II$ )

**Abbreviations**

B–K	Benzeggagh and Kenane fracture criterion
CBBM	compliance based beam method
DCB	double cantilever beam
ENF	end notched flexure
FPZ	fracture process zone
L, R, T	longitudinal, radial and tangential directions of wood
LVDT	linear variable differential transformer
MMB	mixed-mode bending test
SENT	single edge notched tensile

the asymmetrical Wedge Splitting test to determinate the fracture mechanical material properties of spruce under mixed-mode, where the mode I/II ratio ( $G_I/G_{II}$ ) can be changed using asymmetrical wedges with different angles. These tests present an important limitation related to some difficulties in changing the mode ratio in a wide range of values, which is fundamental to obtain a fracture envelop in the  $G_I$ – $G_{II}$  space.

The mixed-mode bending test (MMB) was developed by Reeder and Crews [7] and has been used for mixed-mode I/II interlaminar fracture characterization of artificial composites [8–10]. The test provides an easy variation of the mode ratio only altering the lever length of the loading lever. In this work an MMB test fixture was constructed for fracture characterization of *Pinus pinaster* wood species under mixed-mode I/II loading (Fig. 1), considering the RL crack propagation system. Several experimental tests were performed considering different mode ratios. A data reduction scheme based on beam theory and crack equivalent concept was applied to obtain the fracture energy and the respective mode I and mode II components for the different mode ratios analysed. Numerical analyses were also performed to validate the proposed methodology. It was concluded that the linear fracture criterion is adequate to represent the fracture behaviour of this wood species.

## 2. Experimental tests

The tested material was Maritime pine (*Pinus pinaster* Ait.) wood from the central region of Portugal. All specimens were fabricated from boards of a 2 m part within the stem's tree. The boards were kiln dried in a standard commercial process, and further conditioned at ambient temperature (20–25 °C) and 60–65% relative humidity for at least four weeks. The fracture tests were also performed at these environmental conditions. Real dimensions and mass of each specimen were measured and the density of the tested material was 550 kg m<sup>−3</sup>, for 12.3% moisture content.

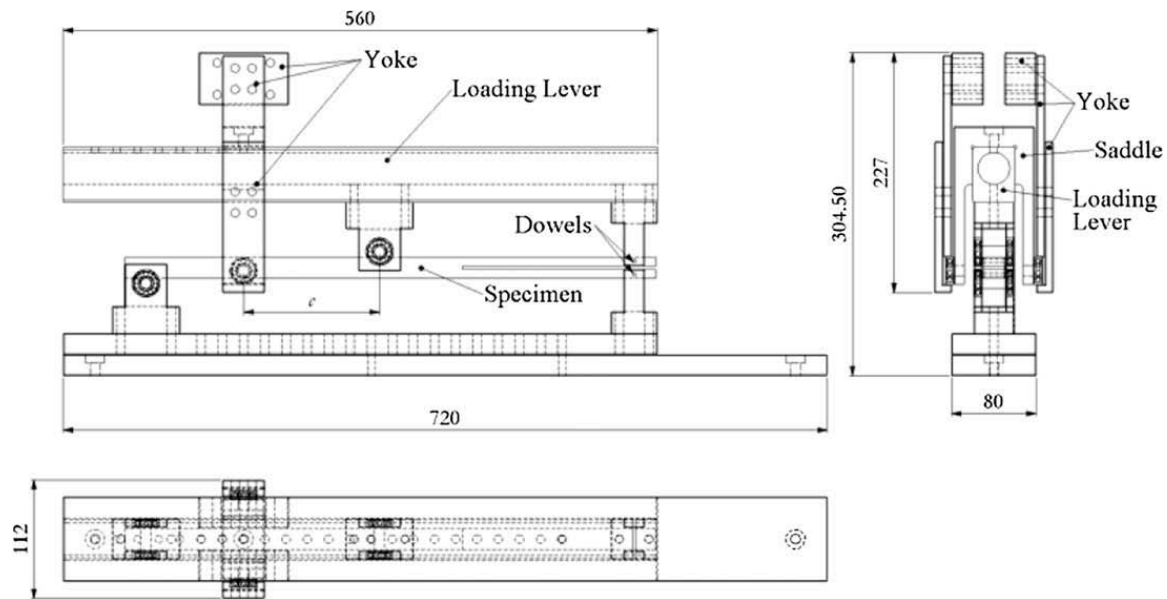


Fig. 1. Schematic representations of the MMB test fixture constructed for wood fracture characterization.

Specimen geometry is represented in Fig. 2a and its dimensions ( $2h = 20$  mm,  $L = 230$  mm,  $L_1 = 250$  mm,  $a_0 = 162$  mm and width  $B = 20$  mm), were based on the authors experience with mode II wood fracture characterization [4,11,12]. A starter crack ( $a_0$ , Fig. 2a) was made just before the fracture tests. First, a 1 mm thickness notch was machined and then a pre-crack of about 2–5 mm was made by a sharp blade. The crack front alignment was verified measuring the initial crack length on both sides of the specimen.

Fig. 2b shows a schematic representation of the MMB test. It should be referred that larger dimensions relatively to the original setup were necessary for this apparatus owing to dimensions of specimens. As a consequence the loading lever is made by aluminium to diminish its weight. The mode ratio can be altered by changing the parameter  $c$  on the loading lever. Ten different mode ratios ( $G_I/G_{II}$ ) were analysed: 0.05, 0.1, 0.15, 0.25, 0.5, 0.75, 1.0, 1.25, 2.0 and 2.75, which is the maximum value allowed with the designed loading rig, due to large specimen dimensions used in wood. Ten tests were performed for each mode ratio and at least seven valid results were obtained.

As already discussed in previous works [3,4,11], crack length monitoring during its growth is very difficult to be performed accurately in wood. Moreover, owing to pronounced fracture process zone (FPZ) developed at the crack tip in wood [3,11], the real crack length can not be considered a truthful parameter to be used in the fracture energy evaluation, since the non negligible amount of energy being dissipated at the FPZ is not accounted for. In order to overcome these issues, the displacements of the two loading points of the loading lever were measured using two LVDT's (linear variable differential transformer), as shown in Fig. 3. These displacements will be used in the proposed data reduction scheme to obtain the fracture

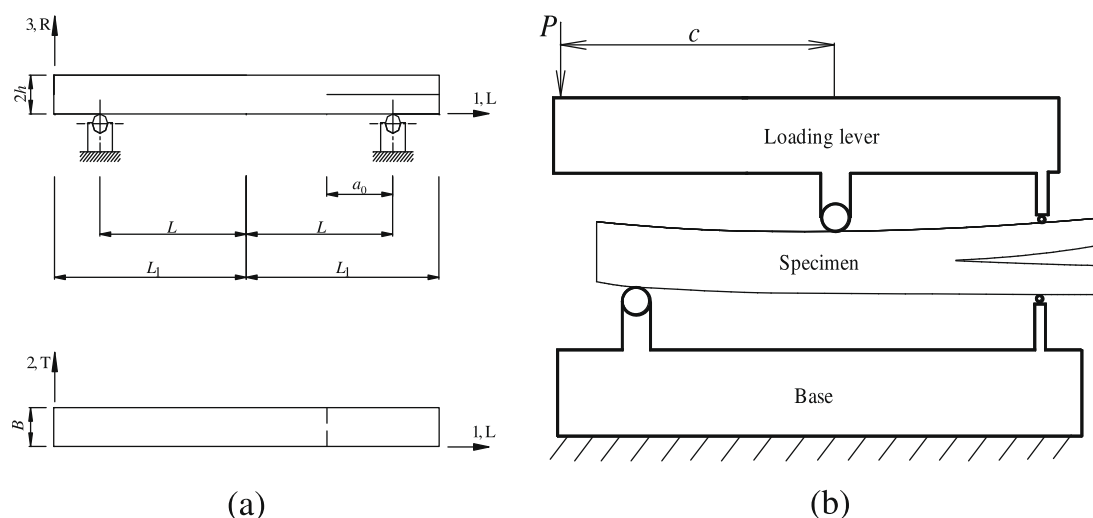


Fig. 2. MMB specimen: (a) geometry; (b) loading conditions.

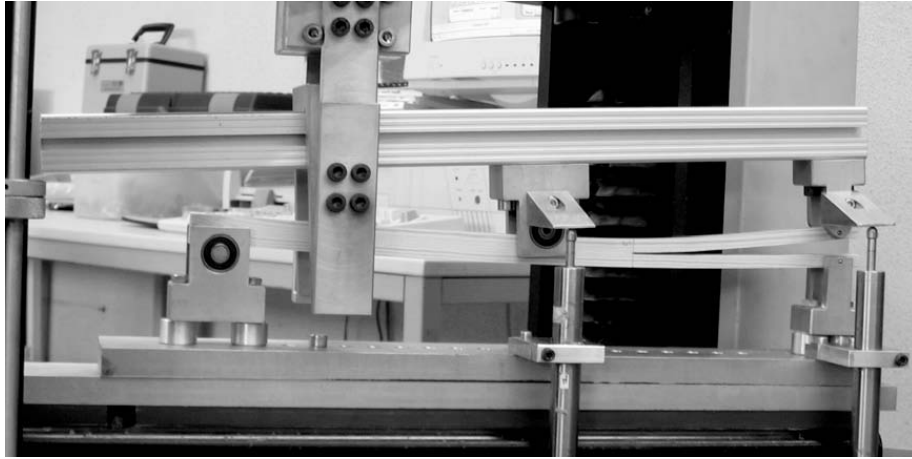


Fig. 3. Experimental setup for the MMB test.

energy without measuring the crack length. Tests were conducted under displacement control using an Instron 1125 testing machine at 5 mm/min displacement rate.

### 3. Mode ratio

The MMB test can be considered as a combination of the double cantilever beam (DCB) and end notched flexure (ENF) tests used for fracture characterization under pure mode I and pure mode II loading, respectively. Following a superposition loading analysis, the mode I and mode II loading components can be written as (Fig. 4)

$$P_I = \left( \frac{3c - L}{4L} \right) P \quad (1)$$

and

$$P_{II} = \left( \frac{c + L}{L} \right) P \quad (2)$$

Simple beam theory can be used to obtain the strain energy release rates in each mode in order to achieve the mode ratio. However, there are some issues that are not accounted for when simple beam theory is applied to DCB and ENF, namely root rotation at the crack tip in the DCB and shear effects in both. Williams [13] proposed a corrected beam theory, where the crack length ( $a$ ) is corrected in order to account for the referred effects. For the DCB test

$$G_I = \frac{12(a + h|\Delta_I|)^2 P_I^2}{B^2 h^3 E_L} \quad (3)$$

and for the ENF [14]

$$G_{II} = \frac{9(a + 0.42h|\Delta_{II}|)^2 P_{II}^2}{16B^2 h^3 E_L} \quad (4)$$

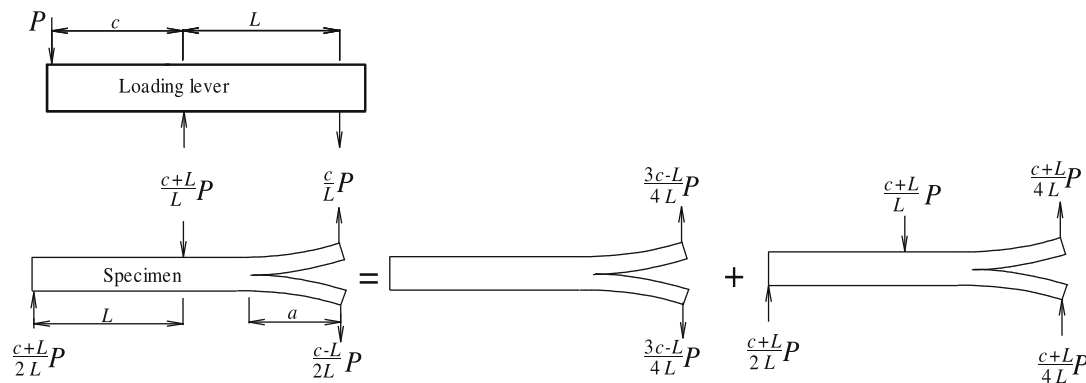


Fig. 4. Superposition loading analysis of the MMB specimen.

being  $E_L$  the longitudinal modulus and  $\Delta_I$  given by

$$\Delta_I = \sqrt{\frac{E_L}{11G_{LR}} \left[ 3 - 2 \left( \frac{\Gamma}{1 + \Gamma} \right)^2 \right]} \quad (5)$$

and

$$\Gamma = 1.18 \frac{\sqrt{E_L E_R}}{G_{LR}} \quad (6)$$

where  $E_R$  and  $G_{LR}$  are the radial and shear modulus, respectively. The mode ratio can be obtained from Eqs. (3) and (4) taking into account relations (1) and (2),

$$\frac{G_I}{G_{II}} = \frac{4}{3} \left( \frac{3c - L}{c + L} \right)^2 \left( \frac{a + h\Delta_I}{a + 0.42\Delta_I h} \right)^2 \quad (7)$$

It was previously verified [15] that this relationship provides a more accurate estimate of mode ratio relatively to the one obtained from simple beam theory.

#### 4. Data reduction scheme

The proposed data reduction scheme was already developed and applied to DCB [3] and ENF [4] tests. It is based on beam theory and crack equivalent concept. The method provides the attainment of resistance curves ( $R$ -curves), thus leading to the accurate measurement of fracture energy. On the other hand, it is not necessary to measure the crack length during propagation, which is very difficult to perform with accuracy in wood. The data reduction is named compliance based beam method (CBBM) since it only depends on the specimen's compliance. The mode I compliance is  $C_I = \delta_I/P_I$ , where  $\delta_I$  is the opening displacement applied by the loading lever at the specimen edge (Fig. 3). Following the Timoshenko beam theory, it can be written [3]

$$C_I = \frac{8a^3}{E_L B h^3} + \frac{12a}{5BhG_{LR}} \quad (8)$$

There are some issues like stress concentrations and root rotation effects at the crack tip influencing the compliance that are not accounted for in the beam theory. On the other hand, it is well-known that the flexural modulus is considerably specimen dependent due to the wood heterogeneity [3,16] which usually requires the previous measurement of the modulus for each specimen. Consequently, a corrected flexural modulus can be estimated from the initials compliance ( $C_{0I}$ ) and crack length ( $a_0$ ) and considering the root rotation effects.

$$E_{fI} = \left( C_{0I} - \frac{12(a_0 + h|\Delta_I|)}{5BhG_{LR}} \right)^{-1} \frac{8(a_0 + h|\Delta_I|)^3}{Bh^3} \quad (9)$$

where  $\Delta_I$  is given by Eqs. (5) and (6) using  $E_{fI}$  instead of  $E_L$ . An iterative process should be used in Eqs. (5), (6), and (9) to obtain a converged value for  $E_{fI}$ .

During crack growth quite extensive FPZ develops at the crack tip. In order to account for the energy being dissipated at this region an equivalent crack in mode I ( $a_{eqI}$ ) can be estimated from the current specimen compliance using Eq. (8). In fact, the FPZ influences the specimen compliance and its effect is thus indirectly accounted for via equivalent crack length. The solution of the cubic equation is obtained using the MATLAB® software [15]. The mode I component is obtained combining the Irwin–Kies equation

$$G = \frac{P^2}{2B} \frac{dC}{da} \quad (10)$$

with Eq. (8), leading to

$$G_I = \frac{6P_I^2}{B^2 h} \left( \frac{2a_{eqI}^2}{h^2 E_{fI}} + \frac{1}{5G_{LR}} \right) \quad (11)$$

A similar procedure can be followed for mode II. The equation of compliance is [4].

$$C_{II} = \frac{3a^3 + 2L^3}{8E_L B h^3} + \frac{3L}{10G_{LR} B h} \quad (12)$$

where  $C_{II} = \delta_{II}/P_{II}$ . The displacement  $\delta_{II}$  is obtained from  $\delta_{II} = \delta_C + \delta_I/4$  [15], being  $\delta_C$  the displacement measured at the specimen mid-span by the loading lever and  $\delta_I$  the displacement measured at the specimen edge. The corrected flexural modulus is obtained using the initials compliance ( $C_{0II}$ ) and crack length ( $a_0$ )

$$E_{II} = \frac{3a_0^3 + 2L^3}{8Bh^3} \left( C_{OII} - \frac{3L}{10G_{LR}Bh} \right)^{-1} \quad (13)$$

The equivalent crack accounting for the FPZ effects can be estimated from Eqs. (12) and (13).

$$a_{eqII} = \left[ \frac{C_{IIcorr}}{C_{OIIcorr}} a_0^3 + \frac{2}{3} \left( \frac{C_{IIcorr}}{C_{OIIcorr}} - 1 \right) L^3 \right]^{1/3} \quad (14)$$

where

$$C_{IIcorr} = C_{II} - \frac{3L}{10G_{LR}Bh} \quad \text{and} \quad C_{OIIcorr} = C_{OII} - \frac{3L}{10G_{LR}Bh} \quad (15)$$

The mode II strain energy release rate component is obtained combining Eqs. (10) and (12).

$$G_{II} = \frac{9P_{II}^2 a_{eqII}^2}{16E_{II} B^2 h^3} \quad (16)$$

Using this method, both components of strain energy release rate under mixed-mode loading can be obtained only from the information given in the  $P$ - $\delta$  curves. The CBBM provides the attainment of  $R$ -curves and does not require crack length monitoring during propagation. Also, it accounts for the FPZ effects, since it is based on current specimen compliance which is influenced by the FPZ. Moreover, it is not necessary to perform previous measurement of the specimen modulus since it is a calculated parameter as a function of initial compliance and crack length. The only parameter needed is the shear modulus  $G_{LR}$ . However, it was verified that it has a minor influence on the results [4] and a typical value can be used.

## 5. Results

During the experimental tests only load–displacement data were recorded to measure the fracture energy under mixed-mode. Since the CBBM is based on specimen compliances in mode I and mode II ( $C_I$  and  $C_{II}$ , respectively), it is necessary to measure the displacements of the specimen at the edge ( $\delta_I$ ) and mid-span ( $\delta_C$ ) induced by the loading lever. This was achieved considering two LVDTs measuring the loading lever applied displacements (Fig. 3). Fig. 5 shows typical load–displacement curves for an intended mode ratio ( $G_I/G_{II}$ ) of 0.5.

The  $R$ -curves for all specimens were obtained considering the described CBBM. In fact, Eqs. (11) and (16) permit the representation of the strain energy components as a function of the respective equivalent crack length. In fact, the plateau values of the  $R$ -curves correspond to self-similar crack propagation, thus allowing an easy identification of each strain energy component (Fig. 6) and the respective mode ratio during crack growth, as well as the total fracture energy under mixed-mode ( $G_{Tc} = G_I + G_{II}$ ).

The average values of fracture energy and its components obtained for each mode ratio are summarized in Table 1. The fourth column shows the standard deviation in percentage for the fracture energy under mixed-mode, considering the valid number of tests (between 7 and 10) for each mode ratio. Large scatter was obtained in the majority of cases. Wood is a natural material with consequent variability in their properties. Moreover, the complex micro-mechanisms of rupture involved during a mixed-mode fracture also contribute to this scatter. Small deviations were also observed in some cases between the measured mode ratios and the intended ones.

The critical fracture energies of this wood species under pure mode loadings were determined in previous works, as being  $G_{Ic} = 0.264$  N/mm [3] and  $G_{IIc} = 0.9$  N/mm [16]. Fig. 7 shows the representation of fracture energy of *Pinus pinaster* wood in  $G_I$

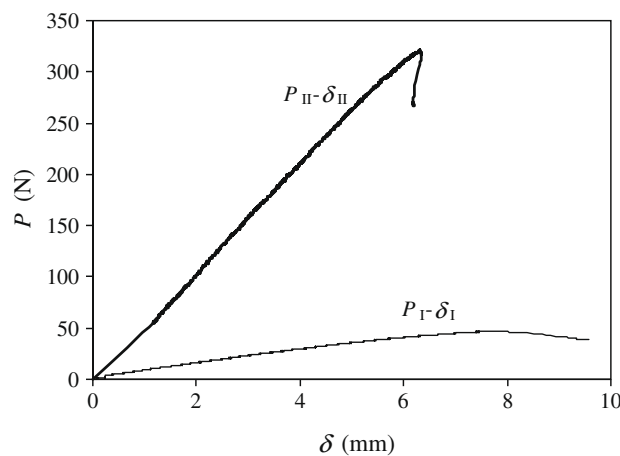


Fig. 5. Typical  $P$ - $\delta$  curves obtained considering an intended mode ratio of 0.5.



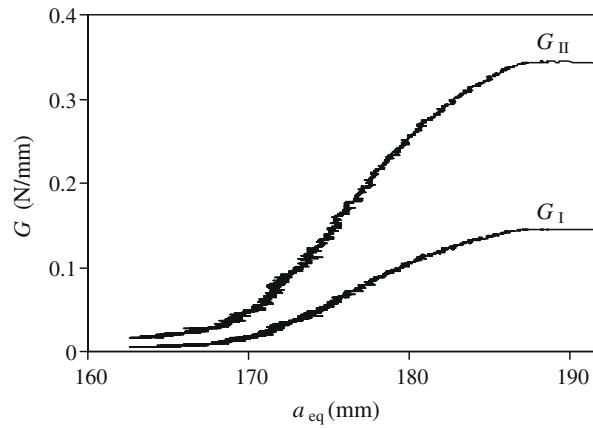


Fig. 6. Typical R-curves obtained considering an intended mode ratio of 0.5.

Table 1

Summary of the MMB experimental results.

$G_I$ (N/mm)	$G_{II}$ (N/mm)	$G_{Tc}$ (N/mm)	$G_{Tc}$ SD (%)	$G_I/G_{II}$ (measured)	$G_I/G_{II}$ (intended)
0.036	0.723	0.759	26.2	0.05	0.05
0.056	0.633	0.690	12.7	0.09	0.1
0.073	0.544	0.616	28.5	0.13	0.15
0.124	0.502	0.626	27.3	0.25	0.25
0.161	0.356	0.517	14.5	0.46	0.5
0.196	0.278	0.474	27.4	0.71	0.75
0.223	0.220	0.443	27.0	1.01	1.0
0.257	0.212	0.469	27.4	1.21	1.25
0.254	0.135	0.389	23.8	1.89	2.0
0.258	0.101	0.359	23.6	2.65	2.75

versus  $G_{II}$  space. This representation includes the referred pure modes and the mixed-mode values measured using the MMB test. Three different fracture criteria were considered in order to characterize the fracture envelop of this wood species. The linear and quadratic criteria are based on the following equation:

$$\left(\frac{G_I}{G_{Ic}}\right)^\eta + \left(\frac{G_{II}}{G_{IIc}}\right)^\gamma = 1 \quad (17)$$

where  $\eta = \gamma = 1$  for the linear and  $\eta = \gamma = 2$  for the quadratic one. The Benzeggagh and Kenane (B-K) criterion [17]

$$G_{Tc} = G_{Ic} + (G_{IIc} - G_{Ic}) + \left(\frac{G_{II}}{G_T}\right)^\eta \quad (18)$$

with  $\eta = 1.5$ , which was verified to be the best fitting value, was also applied. It was observed that for higher values of mode ratio the B-K and quadratic criteria agree with the experimental values. The linear criterion does not perform well for these

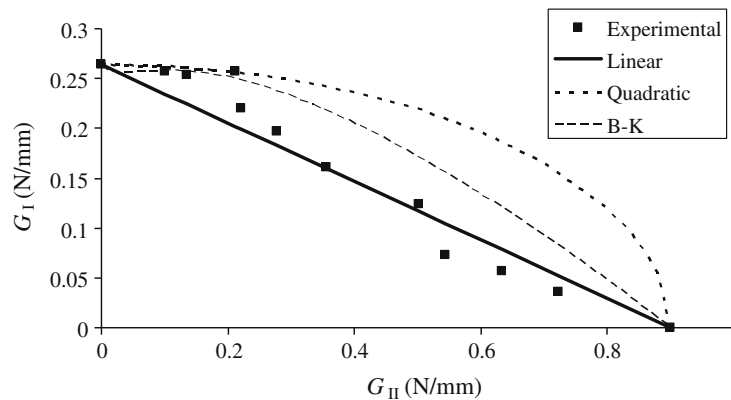


Fig. 7. Representation of fracture energy of *Pinus pinaster* wood in  $G_I$  versus  $G_{II}$  space.



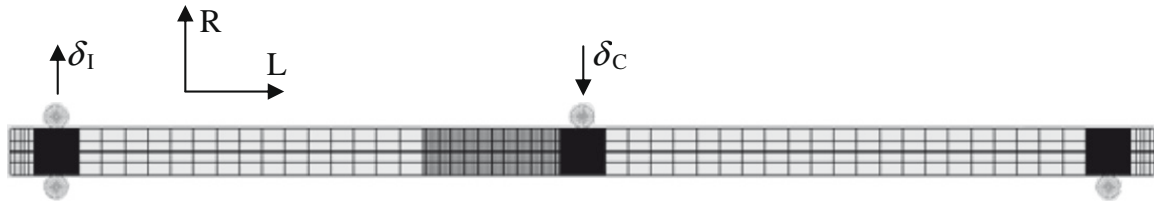
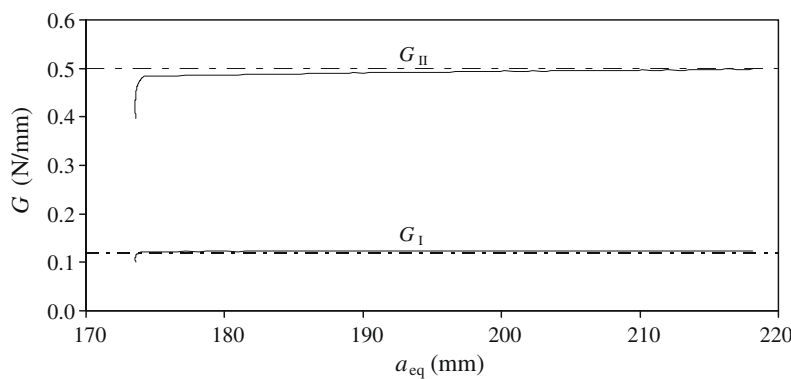


Fig. 8. Mesh of the two-dimensional finite element model.

Table 2

Nominal elastic properties of the *Pinus pinaster* wood [16].

$E_L$ (GPa)	$E_R$ (GPa)	$\nu_{LR}$	$G_{LR}$ (GPa)	$\sigma_{u,R} = \sigma_{u,I}$ (MPa)	$\tau_{u,LR} = \sigma_{u,II}$ (MPa)
12.56	1.91	0.47	1.12	7.93	16.0

Fig. 9. Comparison between the numerical *R*-curves (solid lines) and the average experimental values of strain energy (dashed lines) for  $G_I/G_{II} = 0.25$ .

higher mode ratio values, being conservative. This behaviour is a clear indication that under mixed-mode loading with a small presence of mode II the fracture energy measured in pure mode I practically does not change. As a result, the fracture energy for higher values of mode ratio is similar to  $G_{Ic}$ . This trend is better captured by the quadratic and B–K criteria that present a plateau in this region of  $G_I$ – $G_{II}$  space since the linear one predicts a reduction of fracture energy being conservative. However, globally the linear criterion presents the best performance. In fact, for  $0.05 \leq G_I/G_{II} \leq 1.0$  the linear criterion provides the best agreement with the experimental values, being the other criteria too optimistic.

## 6. Numerical validation

A numerical analysis using cohesive elements was carried out to verify the adequacy of the proposed data reduction scheme on the measurement of fracture energy under mixed-mode loading. A plane strain analysis, considering very refined mesh in the region of crack propagation and contact between specimen and loading/supporting pins, was performed (Fig. 8). The mixed-mode linear softening law is based on the quadratic stress to simulate damage initiation.

$$\left(\frac{\sigma_I}{\sigma_{uI}}\right)^2 + \left(\frac{\sigma_{II}}{\sigma_{uII}}\right)^2 = 1 \quad (19)$$

where  $\sigma_i$  represents the stress in each mode  $i = I, II$  and  $\sigma_{u,i}$  the respective local strength values (see Table 2). Damage growth is simulated when the linear energetic criterion (Eq. (17) with  $\eta = \gamma = 1$ ) is satisfied. The inputted critical fracture energies in pure modes were the ones presented in Fig. 7. A detailed description of the mixed-mode cohesive damage model can be found in [18].

The numerical model was used to validate the CBBM. The case studied corresponds to  $G_I/G_{II} = 0.25$ . In this case, the obtained mode ratio matches the intended one (Table 1). Moreover, its representation in the  $G_I$  versus  $G_{II}$  space complies with the linear energetic criterion (see Table 1 and Fig. 7), used in the numerical simulation. Very small increments and the refined mesh in the region of crack propagation contributed to a smooth crack growth. The CBBM was used to obtain the *R*-curves for each component of strain energy (Eqs. (11) and (16)). Fig. 9 shows the comparison between the numerical and experimental results. As it can be seen, the plateau values of the numerical *R*-curves present excellent agreement with the average strain energy components obtained experimentally.

## 7. Conclusions

In this work fracture characterization of wood under mixed-mode I/II loading was performed using the mixed-mode bending (MMB) test. This test presents an important advantage related to an easy alteration of the mode ratio, which allows a straightforward definition of the fracture envelop in the  $G_I$  versus  $G_{II}$  space. The test apparatus was constructed accounting for the specificities of wood specimens' geometry which implied larger dimensions than the original setup proposed in the literature. Even so, it was concluded that the MMB test is adequate for fracture characterization of wood under mixed-mode I/II loading. A data reduction scheme previously applied to double cantilever beam and end notched flexure tests, was also applied to mixed-mode bending test. The method is based on beam theory and crack equivalent concept presenting several advantages. It is based exclusively on the load–displacement curve and it is named compliance based beam method (CBBM). Using this method, it is not necessary to perform crack length monitoring during propagation which is very difficult to perform accurately in wood. The CBBM also provides the attainment of  $R$ -curves thus making easier the identification of fracture energy. Moreover, with the CBBM it is not necessary to measure previously the longitudinal modulus which varies between different wood specimens. The method was numerically validated using a finite element analysis including a cohesive mixed-mode damage model.

The experimental tests were carried out considering 10 different mode ratios. The CBBM was applied to measure the strain energy components and the corresponding fracture energy under mixed-mode. Three different mixed-mode fracture criteria were applied and it was verified that the linear one presents globally the best performance in reproducing the fracture envelop in the  $G_I$  versus  $G_{II}$  space.

## Acknowledgements

The authors thank the Portuguese Foundation for Science and Technology for supporting the work here presented, through the research project PTDC/EME-PME/64839/2006 and the individual grant SFRH/BD/23893/2005. The authors also thank Professor Alfredo B. de Morais (UA, Portugal) for his advices and discussion about the matters included in this chapter.

## References

- [1] Reiterer A, Sinn G, Stanzl-Tschegg SE. Fracture characteristics of different wood species under mode I loading perpendicular to the grain. *Mater Sci Engng A* 2002;332:29–36.
- [2] Yoshihara H, Ohta M. Measurement of mode II fracture toughness of wood by the end-notched flexure test. *J Wood Sci* 2000;46:273–8.
- [3] de Moura MFSF, Morais JJJ, Dourado N. A new data reduction scheme for mode I wood fracture characterization using the DCB test. *Engng Fract Mech* 2008;75:3852–65.
- [4] de Moura MFSF, Silva MAL, de Morais AB, Morais JJJ. Equivalent crack based mode II fracture characterization of wood. *Engng Fract Mech* 2006;73:978–93.
- [5] Jernkvist LO. Fracture of wood under mixed-mode loading II. Experimental investigation of *Picea abies*. *Engng Fract Mech* 2001;68:565–76.
- [6] Tschegg EK, Reiterer A, Pleschbergers T, Stanzl-Tschegg E. Mixed mode fracture energy of spruce wood. *J Mater Sci* 2001;36:3531–7.
- [7] Reeder JR, Crews JH. Mixed-mode bending method for delamination testing. *AIAA J* 1990;28:1270–6.
- [8] Chen JH, Sernow R, Schulz E, Hinrichsen G. A modification of the mixed-mode bending test apparatus. *Composites Part A* 1999;30:871–7.
- [9] Yum YJ, You H. Pure mode I, II and mixed mode interlaminar fracture of graphite/epoxy composite materials. *J Reinf Plast Compos* 2001;20/09:794–808.
- [10] de Morais AB, Pereira AB. Mixed mode I+II interlaminar fracture of glass/epoxy multidirectional laminates – Part 1: analysis. *Compos Sci Technol* 2006;66:1889–95.
- [11] Silva MAL, Morais JJJ, de Moura MFSF, Lousada JL. Mode II wood fracture characterization using the ELS test. *Engng Fract Mech* 2007;74:2133–47.
- [12] Silva MAL, de Moura MFSF, Morais JJJ. Numerical analysis of the ENF test for mode II wood fracture. *Composites Part A* 2006;37:1334–44.
- [13] Williams JG. End correction for orthotropic DCB specimens. *Compos Sci Technol* 1989;35:367–76.
- [14] Wang Y, Williams JG. Corrections for mode II fracture toughness specimens of composite materials. *Compos Sci Technol* 1992;43:251–6.
- [15] Oliveira JMQ, de Moura MFSF, Morais JJJ, Silva MAL. Numerical analysis of the MMB test for mixed-mode I/II wood fracture. *Compos Sci Technol* 2007;67:1764–71.
- [16] de Moura MFSF, Silva MAL, Morais JJJ, de Morais AB, Lousada JL. Data reduction scheme for measuring  $G_{IIc}$  of wood in end-notched flexure (ENF) tests. *Holzforschung* 2009;63:99–106.
- [17] Benzeggagh ML, Kenane M. Measurement of mixed-mode delamination fracture toughness of unidirectional glass/epoxy composites with mixed-mode bending apparatus. *Compos Sci Technol* 1996;56:439–49.
- [18] de Morais AB, de Moura MFSF, Gonçalves JPM, Camanho PP. Analysis of crack propagation in double cantilever beam tests of multidirectional laminates. *Mech Mater* 2003;35:641–52.